STM JOURNALS

Journal of
Polymer & Composites

ISSN: 2321-2810 (Online)
ISSN: 2321-8525 (Print)
Volume 13, Special Issue 3, 2025
DOI (Journal): 10.37591/JoPC

https://journals.stmjournals.com/jopc

Research JoPC

ANN Approach to Forecasting the Strength of Nano Silica Incorporated Geopolymer Composite

Sagar Paruthi[1,*], Ibadur Rahman[2], Asif Husain[3]

Abstract

Coal and steel industry by-products, such as fly ash (FA) and blast furnace slag (GGBS), have gained significant attention as precursors for geopolymer concrete (GPC) due to their high aluminosilicate content, offering a sustainable alternative to conventional cement. Nano silica (NS), recognized for its exceptional pozzolanic activity and ability to refine microstructure, has shown potential to enhance the mechanical and durability properties of GPC. This study investigates the influence of NS incorporation at varying percentages (1%, 1.5%, 2%) in GPC, cured at different temperatures (27 ^{0}C, 60 ^{0}C, 90 ^{0}C, 120 ^{0}C), on compressive strength (CS), split tensile strength (STS) and flexural strength (FS). Experimental results reveal that GPC cured at 90 ^{0}C for 28 days exhibits the highest strengths i.e. CS of 55.96 MPa, STS of 5.63 MPa, and FS pf 5.66 MPa, demonstrating the effectiveness of heat curing in optimizing mechanical properties. However, the experimental determination of GPC properties is resource intensive. This research introduces machine learning, especially artificial neural networks (ANN), as a predictive tool. The ANN models, trained on 20 GPC mix designs, accurately predict CS (R^2 = 0.9797), STS (R^2 = 0.9847), and FS (R^2 = 0.9864), highlighting their reliability. Compared to traditional modeling approaches, ANN offers superior prediction accuracy, aiding in efficient material proportioning and optimization. The novelty of this research lies in combining advanced nanotechnology and machine learning to address the dual challenges of sustainability and performance in GPC, bridging experimental and computational domains for future infrastructure applications.

Keywords: ANN, nano silica, geopolymer concrete, heat cured, compressive strength

INTRODUCTION

Geopolymers made of aluminosilicate materials were first introduced by Davidovits in 1979 [1]. For manufacturing geopolymers, we used different types of waste from industries like FA from thermal power plants [2], calcium wood ash [3], slag from steel industries [4], rice husk [5], volcanic ash [6] which is used along with an alkaline solution to increase the rate of polymerization [7]. Concrete produced by geopolymerization is environmentally friendly that helps reduce the emission of CO_2 in the atmosphere to a great extent, which comes out during the manufacturing of cement [8]. Geopolymer composites offer several sustainability advantages over conventional cement-based materials. The production of Portland cement is responsible for nearly 8% of global CO_2 emissions [9]. In contrast, geopolymer concrete is made from industrial by-products such as FA and GGBS, significantly reducing the demand for cement and lowering greenhouse gas emissions [10]. Additionally, geopolymer concrete exhibits superior resistance to chemical attack, reduced permeability, and better long-term durability, making it a sustainable alternative in modern construction [11, 12]. Due to the presence of

***Author for Correspondence**
Sagar Paruthi

[1]Assistant Professor, School of Architecture & Design, K. R. Mangalam University, Gurugram, Haryana, India
[2]Assistant Professor, Department of Civil Engineering, Jamia Millia Islamia, New Delhi, India
[3]Professor, Department of Civil Engineering, Jamia Millia Islamia, New Delhi, India

Received Date: November 12, 2024
Accepted Date: February 04, 2025
Published Date: April 25, 2025

Citation: Sagar Paruthi, Ibadur Rahman, Asif Husain. ANN Approach to Forecasting the Strength of Nano Silica Incorporated Geopolymer Composite. Journal of Polymer & Composites. 2025; 13(Special Issue 3): S267–S278p.

aluminosilicate compounds in the byproduct of coal and steel industry i.e., FA and GGBS is significantly used as an alternative to cement concrete [13]. A similar study has been done by Piro et al., in which crushed improvement in the strength of cement concrete is observed after using supplement of crushed stone with GGBS and steel making slag [14]. Sodium hydroxide and sodium silicate rank among the predominant activators employed for the manufacturing of concrete [15]. Mechanical characteristics of GPC are vary with use different type of source material, the basic solution concentration, the amount of sodium silicate, the amount of water, curing time, and curing temperature [16], which are determined in the laboratories as per IS codes. Mix proportion of FA and GGBS based GPC on the basis of activator solution to binder ratio is designed with methodology proposed by reddy et al. [17]. Heat curing is essential in geopolymer concrete development as it accelerates the geopolymerization process, leading to improved mechanical strength and durability. Elevated temperatures enhance the dissolution of aluminosilicate precursors in fly ash and GGBS, resulting in better polymerization and a denser microstructure. Studies indicate that geopolymer composites cured at temperatures between 60°C and 90°C exhibit superior compressive and tensile strength compared to ambient-cured specimens. This research specifically explores the optimal curing temperature for nano silica-modified geopolymer composites, demonstrating that 90°C provides the best strength performance [18]. In addition to performing experiments, various non-destructive methods are available for measuring the CS of GPC [19]. However, these methods require costly equipment and are time-consuming in specimen preparation. For avoiding the time, manpower and cost utilized computation modeling, artificial intelligence (AI) approach [20, 21], multivariable regression model is used to get the correlation of input parameters with mechanical properties of GPC, including ANN, fuzzy interference system (FIS) and neuro fuzzy system (NFS) were used by several researchers [22-33]. ANN with three layers of neurons and fuzzy logic has extensively used in engineering problems due to its capability to solve complexity during the training of the model [34]. It is observed that ANN provides high accuracy prediction with untrained data even when components are limited [13, 35-37]. This research employs three distinct error metrics: mean absolute error (MAE), root mean square error (RMSE), mean absolute percentage error (MAPE), and correlation coefficient (R), to assess the model's effectiveness. The main of this research study is to offer advancement in the existing literature with the help of developing an ANN model for heat-cured nano silica GPC to predict its mechanical properties. During this research, the investigation was done in two phases. The ANN model was trained and validated in the first phase by randomly shuffling the data set in MATLAB. In the second phase accuracy of the model was checked with experimental results. For experimental results, GPC samples were prepared, and testing procedures were applied to determine GPC strength.

MATERIAL & METHODS

Material used in GPC

This study employs two source materials: fly ash (FA), and ground granulated blast furnace slag (GGBS) combination. FA and GGBS are sourced from a thermal power plant and steel plant in Yamuna Nagar, Delhi. Nano Silica (NS), and alkaline activators for GPC concrete is provided by local vendor. Alkaline solution with sodium hydroxide and sodium silicates initiates geopolymerization. The percentage of incorporation of NS and curing temperature are key input parameters impacting GPC properties. Table 1 outlines precursor material oxide percentages along with oxides present in NS. Crushed granite serves as coarse aggregate (CoAg) with varied sizes (7mm, 10mm, 20mm). Badarpur sand is used as fine aggregate (FiAg). The activator solution blends sodium silicate with sodium hydroxide. Table 2 provides physical characteristics of FA, GGBS, FiAg and CoAg.

Table 1. The percentages of oxides present in the source material and NS.

Sample (%)	SiO_2	Fe_2O_3	CaO	Al_2O_3	MgO	K_2O	Na_2O	SO_3	P_2O_5	TiO_2	LOI
FA	49	12.5	2.79	27.25	0.89	0.46	0.32	0.38	0.98	1.54	0.64
GGBS	32.46	0.61	43.1	14.3	3.94	0.33	0.24	4.58	0.02	0.55	0.09
NS	>95.1	-	-	-	-	-	-	-	-	-	-

Table 2. The Physical characteristics of FA, GGBS, FiAg, and CoAg.

Property	FA	GGBS	FiAg	CoAg
Water absorption (%)	-	-	1.2	0.6
Fineness modulus (m^2/kg)	520	408	2.5	7.12
Specific gravity	2.20	3.2	2.6	2.8

METHODOLOGY

Experimental Data

Twenty mix proportions were designed, and for every mix proportion, nine specimens were prepared, out of which three were for CS, three specimens for STS, and three for FS determination of GPC. One day of heat curing in an oven is followed by additional curing at ambient temperature until the day of performing test. Strength is determined after 28 days curing. Detailed information about the material components, specimen mix preparation, and data collection is presented in sub-sections

Specimen Preparation

Specimens of GPC were prepared with a mix design procedure using IS 10262-2009 and IS 456: 2005. The source material, sand, and CoAg used in the mix for the production of concrete were in the ratio 1:1.28: 2.99. The concentration of NaOH used for preparing the alkaline solution was 16M. The exothermic reaction occurs when we add NaOH to water, so this solution was ready 1 day before the day of casting. Sodium naphthalene formaldehyde-based superplasticizer was useful to enhance the workability. Superplasticizer was employed in an amount equal to 1.5% of the binding material. For specimen preparation, the aggregate was mixed and blended in a mixer for 1 min. Then, FA is put into a mixer and blended with aggregate for 3-5 min. After this, GGBS is mixed and blended for 2 min. After this, NS are put into a mixer and blended for 2 minutes. After this, the superplasticizer is put into a mixer and blended for 1 min. Subsequently, the amalgamated solution of sodium hydroxide and sodium silicate was introduced into the mixer and blended for duration of 4 to 6 minutes. The proportion of NaOH/ Na_2SiO_3 used was 2.5 for all the mixtures. The cubical specimen of 150 x 150 x 150 mm, cylindrical specimen of 200 x 100 mm, and prism specimen of 500 x 100 x 100 mm size were prepared to determine the CS, STS, and FS of concrete. Using a compression testing equipment with a 2000 KN capacity and a constant loading rate, the strength were calculated (see Figure 1). According to the guidelines of IS 516:1959. the compressive strength of GPC specimens was determined. According to IS 5816:1999 and IS 516:1959, the STS and FS of the GPC specimen were computed. The proportion of different materials used in producing GPC incorporated with different percentage of NS and cured at different temperature is listed in Table 3.

Figure 1. Compressive strength test of specimens under compression testing machine

Table 3. The proportion of different materials used in producing GPC (Kg/m^3).

Mix	FA	GGBS	NaOH	Na_2SiO_3	SP	CoAg	FiAg
GPC	213.1	213.1	42.6	106.6	6	1276.8	547.8

Artificial Neural Network

Inputs with their weights, functions for sum and activation, and the target output are the major elements of the architecture of an artificial neural network [38). Eq.1 is used for weighted and summing the input in the artificial neural network.

$$y = f(\sum_{i=0}^{n} x_i w_i - b) \quad (1)$$

Where activation function is represented by 'f' and input neuron, and their corresponding weight is represented by 'x_i' & 'w_i' respectively. In Eq. (1), the bias term and the number of neurons are denoted by 'b' and 'n', respectively. The target output is represented by y in Eq. 1. In Eq. 1, activation function 'f' is applied to the input given by $(\sum_{i=0}^{n} x_i w_i - b)$. In Artificial Neural Network during multi-layer feed-forward operation, the function used for activation is Sigmoidal, which has 'S-shaped' curve, and Eq.(2) represents the sigmoidal function mathematically [39).

$$f(t) = \frac{1}{1+ e^{-\alpha t}} \; where \; t = \sum_{i=0}^{n} x_i w_i - b) \quad (2)$$

In Eq. (2), the semi-linear region gradient is managed by constant 'α'. The network forwards the signals continuously again and again to achieve closed output. If there is a difference between predicted and calculated outcomes, then this difference value is sent back to the input from output to distribute this error in all neurons equally. The weights are continuously updated based on these back-propagated signals. The ANN structure formulated within this study are shown in Figures.

Model Performance Determination

The most widely used technique for concrete strength prediction in the machine learning approach is ANN [40). Due to high performance efficiency of ANN model among all AI models, ANN is extensively used in many engineering problems [9, 41). For better estimation of the GPC specimen strength, ANN network should be well-trained. Test results were classified into two subdivisions, the primary division is for training both models, and the secondary division is for testing both models. Three different categories of error, RMSE, MAE, and MAPE, were used in this research to examine the performance effectiveness of the ANN model. It was also observed that forecasting results are better with lower values of RMSE and MAE [42). MAE measures errors between paired observations expressing the same phenomenon and is given by eq. (3). MAPE for GPC strength prediction is given by eq. (4). RMSE for GPC strength prediction can be calculated by eq. (5).

In the present research, a three-layer perceptron ANN model based on a subtractive cluster algorithm was created with the help of MATLAB (2018) for GPC specimens strength prediction. The three major components of artificial neural networks are the input, output, and computational layers. Two different parameters i.e., percentage of nano silica and curing temperature, were considered input parameters. The target output is types of strength of GPC. In this study, the Levenberg-Marquardt algorithm is used in ANN analysis. The range of parameters of the ANN model is shown in Table 4. During the model's training, we need to change the value of the number of neurons and number of hidden layers until the model's outcome is closer to the outcome of the experiments. The experimental result is divided into two parts, out of which one part was used to train the model, and another part checks the model's accuracy. The experimental data considered for training the model consist of results of GPC specimens cured at 60 ˚C, 90 ˚C, and 120 ˚C, and the experimental data considered for testing the model consists of results of GPC specimens cured at 27 ˚C and 75 ˚C. During the training phase of the model, better prediction is yielded at three hidden layers with six neurons. So, for testing the prediction of strength results of GPC specimens, three hidden layers with six neurons were used in the ANN.

$$\text{MAE} = \frac{1}{n}\sum_{i=1}^{n}|x_i - y_i| \quad (3)$$

$$\text{MAPE} = \frac{100}{n}\sum_{i=1}^{n}\frac{|x_i - y_i|}{x_i} \quad (4)$$

$$\text{RMSE} = \sqrt{\left(\frac{1}{n}\right)\sum_{i=1}^{n}|x_i - y_i|^2} \quad (5)$$

Where x_i, y_i and n are the experimental, predicted, and number of values, respectively.

Table 4. The range of parameters of the ANN model.

S N.	Characteristic	Range	Type of parameters
1	Nano silica (%)	0-2	Input
2	Curing temperature (˚C)	27-120	Input
3	CS (MPa)	42.9-55.96	Output
4	FS (MPa)	4.32-5.66	Output
5	STS (MPa)	4.75-5.63	Output

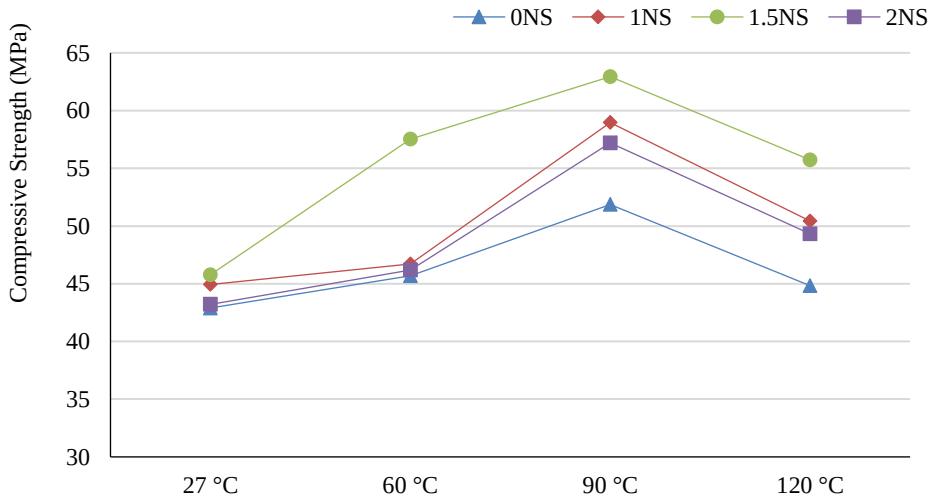

Figure 2. 28-days compressive strength alterations at various curing temperatures.

RESULTS AND DISCUSSION

Compressive Strength

The change in GPC CS cured for 28 days under different temperatures of curing for 1 day is shown in Figure 2. During all the percentages of NS considered, compressive strength rises with rises in temperature of curing of GPC up to 90 ˚C. GPC compressive strength is increased with 90 ˚C temperature of curing is 20.88%, 31.22%, 37.48%, and 32.37% as in comparison with GPC compressive strength at 27 ˚C respectively for 0%, 1%, 1.5%, and 2% use of NS. It was also noted that the strength of GPC is increases with an increase in the percentage of incorporation of NS in GPC up to 1.5%.

At 27 ˚C the CS of GPC is increased by 4.73%, 6.71%, and 0.77% with the incorporation of 1%, 1.5%, and 2% NS respectively in comparison with 0%NS GPC. A similar effect of the dosage of NS on the CS is observed for all the curing temperatures. It was also noticed from the results that for all the curing temperatures the highest strength is observed after incorporation of 1.5% NS in GPC. These observations indicate that GPC strength is influenced by the temperature of curing and the dosage of NS incorporated as well.

Split Tensile Strength

Figure 3 depicts how the GPC split tensile strength (STS) changed at various curing temperatures after curing for 28 days. The relationship between STS and curing temperature is comparable to that

between CS and curing temperature. STS increases with higher curing temperatures, up to 90 °C, for all NS (%) characteristics. The percentage rise in STS of GPC specimens with 90 ˚C curing temperature is 23.05%, 23.83%, 31.62%, and 20.37%, respectively, compared to tensile strength at 27 ˚C for 0%, 0.5%, 1%, and 1.5% use of NS. It was also noticed that the split tensile strength of GPC (N0C27, N0.5C27, N1C27, N1.5C27) with 27 ˚C curing temperature and that of GPC specimens (N0C90, N0.5C90, N1C90, N1.5C90) with 90 ˚C curing temperature varied much. It was also noted that the STS of GPC increases with an increase in the percentage of incorporation of NS in GPC up to 1.5%.

At 27 ˚C the STS of GPC is increased by 0.70%, 1.17%, and 0.47% with the incorporation of 1%, 1.5%, and 2% NS respectively in comparison with 0%NS GPC. A similar effect of the dosage of NS on the STS is observed for all the curing temperatures.

Flexural Strength

In Figure 4, it is depicted how the GPC's flexural strength changes as it is cured at various temperatures. It was noticed that variation in the GPC flexural strength is also similar to variation in the other two strengths. It was noticed from the experimental results that for 2% NS, flexural strength is not increased much with increased temperature of curing. The percentage increase in flexural strength under 90 ˚C curing was observed to be within the limit for all nano silica (%), the same as the limit increase in split tensile strength for all NS (%). The percentage rise of GPC strength in flexural is the same as in compression at 90 ˚C curing as compared to the 27 ˚C curing is 12.89%, 15.17%, 16.08%, and 13.95%, respectively for 0%, 0.5%, 1%, and 1.5% NS. Similar to the other two strength test results, test results show that the flexural strength of GPC specimens (N0C27, N0.5C27, N1C27, N1.5C27) at 27 ˚C curing temperature and that of GPC specimens (N0C90, N0.5C90, N1C90, N1.5C90) at 90 ˚C curing temperature did not differ significantly.

It was also noted that the FS of GPC increases with an increase in the percentage of incorporation of NS in GPC up to 1.5%. At 27 ˚C the FS of GPC is increased by 1.69%, 2.53%, and 1.47% with the incorporation of 1%, 1.5%, and 2% NS respectively in comparison with 0%NS GPC. A similar effect of the dosage of NS on the FS is observed for all the curing temperatures.

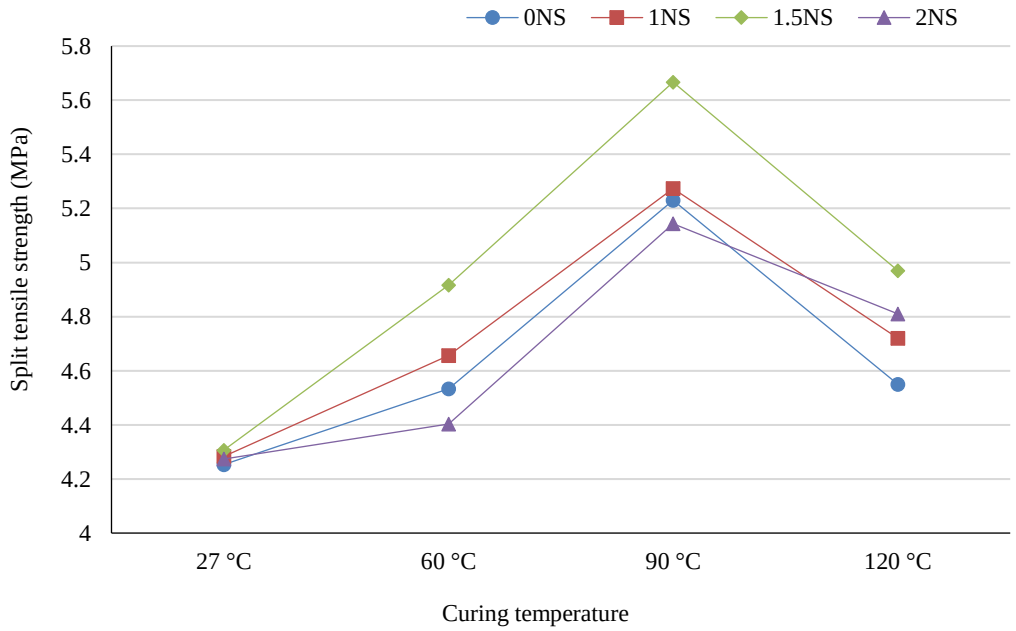

Figure 3. The change in 28 days split tensile strength under different temperatures of curing.

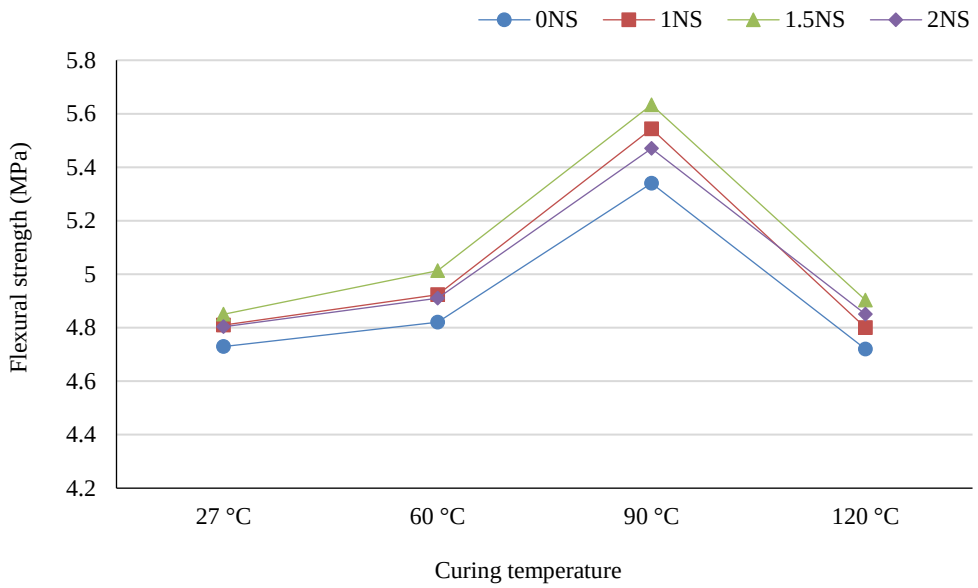

Figure 4. The change in flexural strength under different temperatures of curing.

Effect of Heat Curing on Strength Characteristics

The experimental results demonstrate a clear correlation between heat curing conditions and the mechanical properties of geopolymer composites. Compressive strength, split tensile strength, and flexural strength increase with curing temperature up to 90°C but decline beyond this point. At 27°C, the compressive strength of GPC was 42.9 MPa, which increased by approximately 31.22% when cured at 90°C, reaching 55.96 MPa. However, further increasing the curing temperature to 120°C led to a decline in strength due to excessive moisture loss, causing microcracks. A similar trend was observed for STS and FS. The highest STS (5.63 MPa) and FS (5.66 MPa) were recorded at 90°C, with a subsequent decline at 120°C. These findings suggest that heat curing is necessary to achieve optimal strength in geopolymer concrete but must be controlled to prevent microstructural defects caused by high-temperature-induced moisture evaporation.

Model Performance

The effectiveness of constructed ANN model is improved by using indicators like coefficient of correlation (R), MAE, RMSE, and MAPE. Table 5 displays the values of indicators for various ANN model output parameters. The indicators in Table 5 showed that the ANN model performed well in predicting GPC strength, with values of R^2 of 0.9797 for compressive strength, 0.9847 for split tensile strength, and 0.9864 for flexural strength, respectively. The performance of ANN model can also be represented by regression plots. Fig. 5, 6, and 7 illustrates the effectiveness of the constructed ANN model using the provided input dataset in predicting the compressive, split tensile, and flexural strength respectively. MAPE value represents the mean absolute percentage error for GPC strength prediction, which is 0.45% for CS prediction. For predicting STS and FS, its MAPE is 1.51% and 0.84%, respectively, during the use of the ANN model. The variance between ANN-based forecasts and real experimental outcomes is shown in Table 6.

Table 5. Performance results of the ANN model.

Parameters	R^2	MAE	RMSE	MAPE
Compressive strength	0.9797	0.2546	0.05574	0.45
Split tensile strength	0.9847	0.0954	0.1043	1.51
Flexural strength	0.9864	0.06125	0.0884	0.84

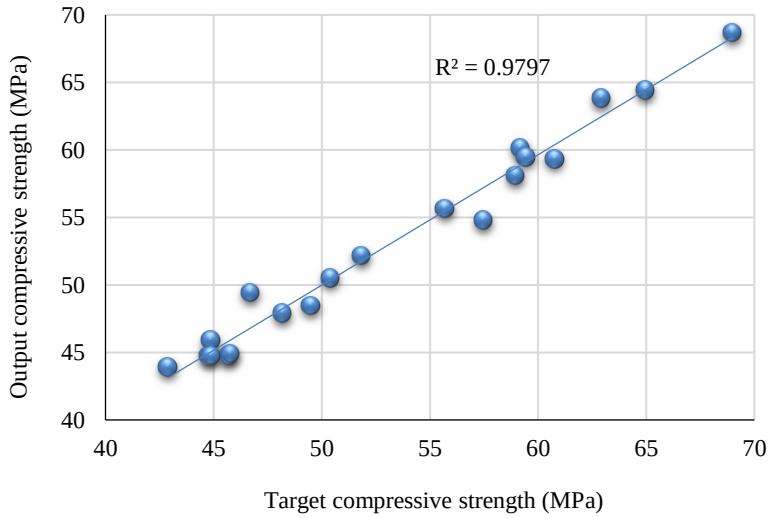

Figure 5. Regression plot of developed ANN model for compressive strength prediction.

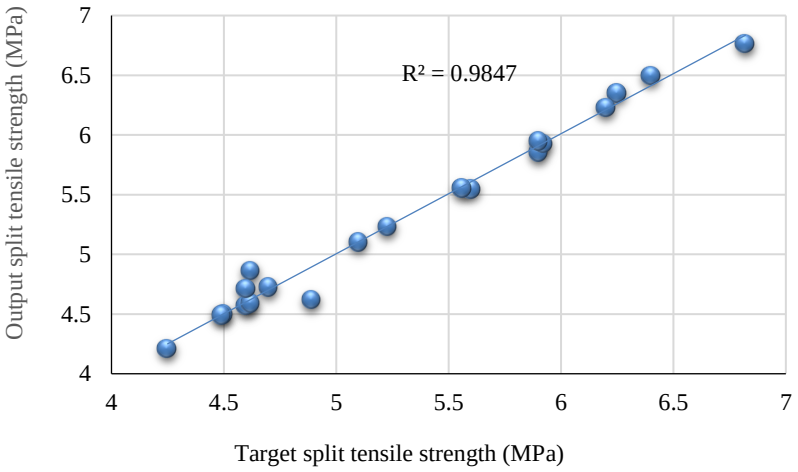

Figure 6. Regression plot of developed ANN model for split tensile strength prediction.

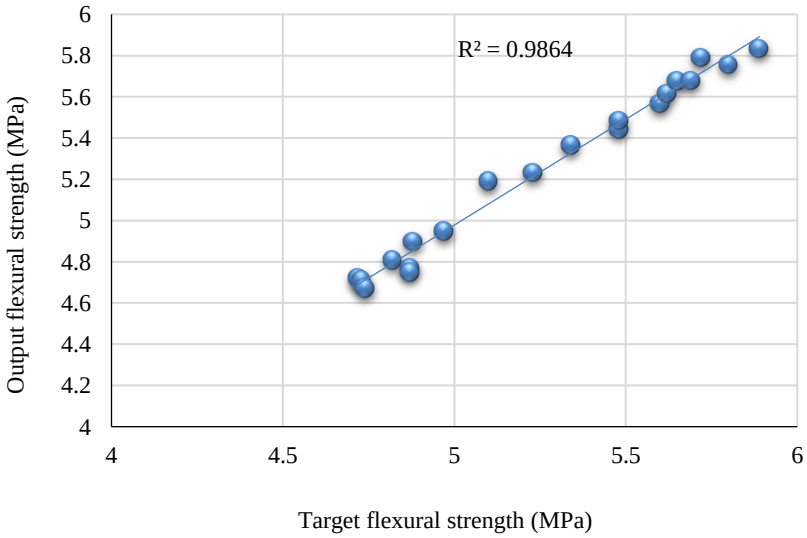

Figure 7. Regression plot of developed ANN model for flexural strength prediction.

Table 6. Comparison between the predicted and experimental using ANN.

S N.	Mix	CS (MPa)			STS (MPa)			FS (MPa)		
		Exp.	*Pred.*	*Error (%)*	*Exp.*	*Pred.*	*Error (%).*	*Exp.*	*Pred.*	*Error (%).*
1	N0C27	42.9	41.91	-2.3	4.25	4.28	0.9	4.73	4.74	0.4
2	N0C60	45.7	46.61	2.0	4.53	4.53	0.2	4.82	4.83	0.4
3	N0C90	51.86	51.60	-0.5	5.23	5.23	0.1	5.34	5.32	-0.3
4	N0C120	44.83	44.87	0.1	4.55	4.55	0.2	4.72	4.73	0.2
5	N1C27	44.93	43.94	-2.2	4.28	4.30	0.6	4.81	4.92	2.4
6	N1C60	46.72	44.05	-5.7	4.65	4.63	-0.4	4.92	4.91	-0.2
7	N1C90	58.96	59.84	1.5	5.27	5.23	-0.6	5.54	5.54	0
8	N1C120	50.42	50.36	-0.1	4.72	4.72	0	4.8	4.8	0
9	N1.5C27	45.78	46.64	1.9	4.30	4.32	0.6	4.85	4.91	1.4
10	N1.5C60	57.53	60.23	4.7	4.91	4.95	1	5.01	5.04	0.7
11	N1.5C90	62.94	62.31	-1	5.66	5.56	-1.6	5.63	5.57	-1
12	N1.5C120	55.72	55.77	0.1	4.97	4.97	0.1	4.90	4.90	0.1
13	N2C27	43.21	43.46	0.6	4.27	4.50	5.5	4.80	4.71	-1.7
14	N2C60	46.2	45.46	-1.6	4.40	4.38	-0.3	4.91	4.89	-0.3
15	N2C90	57.2	57.42	0.4	5.14	5.18	0.8	5.47	5.52	1
16	N2C120	49.33	49.37	0.1	4.81	4.81	0	4.85	4.88	0.7

CONCLUSION

Here, we examine the ANN approach to AI, which seeks to forecast the three forms of GPC strength. The percentage of NS and curing temperature are the two-input parameters used in this study. However, we considered three different types of strength as output parameters. The prediction performance of the AI system was examined using the coefficient of correlation (R), MSE, RMSE, and MAPE. Upon conducting both the model-based and experimental investigation outlined in this paper, the subsequent conclusion can be inferred:

1. It was observed that the Levensberg Marquardt algorithm used in Artificial neural networks performs better in predicting all types of GPC strength.
2. It was noticed that the developed ANN model works well in predicting all three types of strength of GPC with the highest R^2 for compressive strength (0.9797), split tensile strength (0.9847), and flexural strength (0.9864). The efficiency of the developed ANN model is reliable with minimum error for compressive strength prediction (MAE = 0.2546, RMSE = 0.05574, MAPE = 0.45), split tensile strength prediction (MAE = 0.0954, RMSE = 0.1043, MAPE = 1.51) and flexural strength prediction (MAE = 0.06125, RMSE = 0.0884, MAPE = 0.84) of GPC cured under different temperature conditions.
3. Mechanical properties of GPC were improved and enhanced with the increase in the NS percentage for all the temperature conditions up to an optimum percentage of NS.
4. Mechanical properties of GPC were improved and enhanced with the increase in the temperature of curing up to 90 ˚C. However, beyond 90 ˚C, it led to a decline.
5. High-strength GPC is achieved after adding up to 1.5% NS, even at ambient curing conditions.
6. Incorporating FA, GGBS in the ratio 50FA:50GGBS gives a sustainable GPC composite.
7. ANN approach outperformed predicting the strength of concrete due to its easy adaptability. This method can also be used in the prediction of the durability of GPC. We can also plan to study the different machine learning algorithms to compare the prediction of strength of nanomaterial incorporated GPC using different AI approaches.
8. The research findings highlight the sustainability benefits of geopolymer composites. The use of industrial waste materials (FA and GGBS) in place of cement significantly reduces carbon emissions. Unlike traditional concrete, which emits large amounts of CO_2 during cement

production, geopolymer concrete utilizes existing waste materials, contributing to a circular economy. Additionally, the ANN-based predictive modeling used in this study optimizes mix proportions, reducing the need for excessive material usage and experimental trials, thereby lowering environmental impact.

9. Overall, the combination of nanomaterial incorporation and machine learning techniques presents a viable pathway for promoting low-carbon and energy-efficient construction materials.

REFERENCES

1. Davidovits J, Cordi S. Synthesis of new high temperature geo-polymers for reinforced plastics/composites. Spe Pactec. 1979;79:151-4.
2. Garg R, Garg R, Eddy NO, Khan MA, Khan AH, Alomayri T, et al. Mechanical strength and durability analysis of mortars prepared with fly ash and nano-metakaolin. Case Studies in Construction Materials. 2023;18:e01796.
3. Ma C-K, Awang AZ, Omar W. Structural and material performance of geopolymer concrete: A review. Construction and Building Materials. 2018;186:90-102.
4. Shahmansouri AA, Bengar HA, Ghanbari S. Compressive strength prediction of eco-efficient GGBS-based geopolymer concrete using GEP method. Journal of Building Engineering. 2020;31:101326.
5. Nazari A, Bagheri A, Riahi S. Properties of geopolymer with seeded fly ash and rice husk bark ash. Materials Science and Engineering: A. 2011;528(24):7395-401.
6. Alraddadi S, Assaedi H. Characterization and potential applications of different powder volcanic ash. Journal of King Saud University-Science. 2020;32(7):2969-75.
7. Palomo A, Grutzeck M, Blanco M. Alkali-activated fly ashes: A cement for the future. Cement and concrete research. 1999;29(8):1323-9.
8. Alekhya P, Aravindan S. Experimental investigations on geopolymer concrete. Int J Civ Eng Technol (IJCIET). 2014;5(4):01-9.
9. Paruthi S, Husain A, Alam P, Khan AH, Hasan MA, Magbool HM. A review on material mix proportion and strength influence parameters of geopolymer concrete: Application of ANN model for GPC strength prediction. Construction and Building Materials. 2022;356:129253.
10. Paruthi S, Rahman I, Husain A, Hasan MA, Khan AH. Effects of chemicals exposure on the durability of geopolymer concrete incorporated with silica fumes and nano-sized silica at varying curing temperatures. Materials. 2023;16(18):6332.
11. Paruthi S, Rahman I, Husain A, Khan AH, Manea-Saghin A-M, Sabi E. A comprehensive review of nano materials in geopolymer concrete: Impact on properties and performance. Developments in the Built Environment. 2023;16:100287.
12. Paruthi S, Rahman I, Khan AH, Sharma N, Alyaseen A. Strength, durability, and economic analysis of GGBS-based geopolymer concrete with silica fume under harsh conditions. Scientific Reports. 2024;14(1):31572.
13. Nagajothi S, Elavenil S. Influence of aluminosilicate for the prediction of mechanical properties of geopolymer concrete–artificial neural network. Silicon. 2020;12(5):1011-21.
14. Piro NS, Mohammed AS, Hamad SM. Evaluate and predict the resist electric current and compressive strength of concrete modified with GGBS and steelmaking slag using mathematical models. Journal of Sustainable Metallurgy. 2023;9(1):194-215.
15. Kong DL, Sanjayan JG. Damage behavior of geopolymer composites exposed to elevated temperatures. Cement and Concrete Composites. 2008;30(10):986-91.
16. Davidovits J. Synthetic mineral polymer compound of the silicoaluminates family and preparation process. Google Patents; 1984.
17. Reddy MS, Dinakar P, Rao BH. Mix design development of fly ash and ground granulated blast furnace slag based geopolymer concrete. Journal of Building Engineering. 2018;20:712-22.
18. Paruthi S, Khan AH, Isleem HF, Alyaseen A, Mohammed AS. Influence of silica fume and alccofine on the mechanical performance of GGBS-based geopolymer concrete under varying curing temperatures. Journal of Structural Integrity and Maintenance. 2025;10(1):2447661.

19. Huynh AT, Nguyen QD, Xuan QL, Magee B, Chung T, Tran KT, et al. A machine learning-assisted numerical predictor for compressive strength of geopolymer concrete based on experimental data and sensitivity analysis. Applied Sciences. 2020;10(21):7726.
20. Kaliraman B, Verma R, Paruthi S. Internet of things in sustainable concrete production. Recent Developments and Innovations in the Sustainable Production of Concrete: Elsevier; 2025. p. 621-33.
21. Verma R, Kaliraman B, Paruthi S. Machine learning in concrete construction: applications, challenges, and future aspects. Recent Developments and Innovations in the Sustainable Production of Concrete: Elsevier; 2025. p. 577-93.
22. Lin Y, Lai C-P, Yen T. Prediction of ultrasonic pulse velocity (UPV) in concrete. Materials Journal. 2003;100(1):21-8.
23. Dao DV, Ly H-B, Trinh SH, Le T-T, Pham BT. Artificial intelligence approaches for prediction of compressive strength of geopolymer concrete. Materials. 2019;12(6):983.
24. Dao DV, Trinh SH, Ly H-B, Pham BT. Prediction of compressive strength of geopolymer concrete using entirely steel slag aggregates: Novel hybrid artificial intelligence approaches. Applied Sciences. 2019;9(6):1113.
25. Nguyen KT, Nguyen QD, Le TA, Shin J, Lee K. Analyzing the compressive strength of green fly ash based geopolymer concrete using experiment and machine learning approaches. Construction and Building Materials. 2020;247:118581.
26. Ling Y, Wang K, Wang X, Li W. Prediction of engineering properties of fly ash-based geopolymer using artificial neural networks. Neural Computing and Applications. 2021;33(1):85-105.
27. Kheder G. A two stage procedure for assessment of in situ concrete strength using combined non-destructive testing. Materials and Structures. 1999;32(6):410-7.
28. Trtnik G, Kavčič F, Turk G. Prediction of concrete strength using ultrasonic pulse velocity and artificial neural networks. Ultrasonics. 2009;49(1):53-60.
29. Ahmad M, Rashid K, Tariq Z, Ju M. Utilization of a novel artificial intelligence technique (ANFIS) to predict the compressive strength of fly ash-based geopolymer. Construction and Building Materials. 2021;301:124251.
30. Yadollahi MM, Benli A, Demirboga R. Application of adaptive neuro-fuzzy technique and regression models to predict the compressive strength of geopolymer composites. Neural Computing and Applications. 2017;28:1453-61.
31. Garg A, Aggarwal P, Aggarwal Y, Belarbi M, Chalak H, Tounsi A, et al. Machine learning models for predicting the compressive strength of concrete containing nano silica. Computers and Concrete. 2022;30(1):33.
32. Paruthi S, Rahman I, Husain A. Utilizing ANFIS for strength characteristics forecasting in variable heat-cured geopolymer composites. Materials Today: Proceedings. 2024.
33. Paruthi S, Rahman I, Husain A. Comparative studies of different machine learning algorithms in predicting the compressive strength of geopolymer concrete. Computers and Concrete. 2023;32(6):607.
34. Kumari P, Paruthi S, Alyaseen A, Khan AH, Jijja A. Predictive performance assessment of recycled coarse aggregate concrete using artificial intelligence: A review. Cleaner Materials. 2024:100263.
35. Elshafey AA, Dawood N, Marzouk H, Haddara M. Crack width in concrete using artificial neural networks. Engineering structures. 2013;52:676-86.
36. Jiang G, Keller J, Bond PL, Yuan Z. Predicting concrete corrosion of sewers using artificial neural network. Water research. 2016;92:52-60.
37. Emad W, Mohammed AS, Bras A, Asteris PG, Kurda R, Muhammed Z, et al. Metamodel techniques to estimate the compressive strength of UHPFRC using various mix proportions and a high range of curing temperatures. Construction and Building Materials. 2022;349:128737.
38. Kong X, Khambadkone AM. Modeling of a PEM fuel-cell stack for dynamic and steady-state operation using ANN-based submodels. IEEE Transactions on Industrial Electronics. 2009;56(12):4903-14.

39. Anderson JA. Cognitive and psychological computation with neural models. IEEE transactions on systems, man, and cybernetics. 1983(5):799-815.
40. Golafshani EM, Behnood A, Arashpour M. Predicting the compressive strength of normal and High-Performance Concretes using ANN and ANFIS hybridized with Grey Wolf Optimizer. Construction and Building Materials. 2020;232:117266.
41. Azadeh A, Seif J, Sheikhalishahi M, Yazdani M. An integrated support vector regression–imperialist competitive algorithm for reliability estimation of a shearing machine. International Journal of Computer Integrated Manufacturing. 2016;29(1):16-24.
42. Paruthi S, Khan AH, Kumar A, Kumar F, Hasan MA, Magbool HM, et al. Sustainable cement replacement using waste eggshells: A review on mechanical properties of eggshell concrete and strength prediction using artificial neural network. Case Studies in Construction Materials. 2023;18:e02160.

